Tribology of novel antibiocorrosion coatings

Kh. Barbakadze[1,2], W. Brostow*[1], N. Hnatchuk[1], Z. Hoyt[1] and N. Lekishvili[2]

We have developed inorganic–organic hybrid bioactive composites and antibiocorrosion coatings based on epoxy or polyurethane matrices modified with varying amounts of a silicon organic oligomer. We have incorporated bioactive compound containing bis(η^5-cyclopentadienyl) iron and spatial alicyclic fragment or its coordination compounds of Co and Ni. Glass transition regions located with differential scanning calorimetry (DSC) are above $+50^{\circ}$C, so that our hybrids can be used for instance as coatings for museum exhibits. DSC shows also beta transitions in the glassy state around -50°C. Thermogravimetric analysis shows high thermal stability. We have also performed scratch resistance testing with linearly increasing load and sliding wear determination by multiple scratching along the same groove. Also here the hybrid formation enhances the scratch resistance. We observe the strain hardening in sliding wear that is the tendency towards a horizontal groove depth asymptote with increasing number of scratches. Water absorption in 720 h does not exceed 0·03 wt-% in all cases. Samples subjected to three months aging under normal temperature and pressure conditions were observed. The initial colours and optical transparency were preserved; no phase separation took place.

Keywords: Hybrid, Epoxy, Siloxane, Polyurethane, Scratch resistance, Sliding wear

Introduction

The growing population of aggressive microorganisms provoked by deterioration of ecological conditions stimulates a series of biocorrosive processes that cause huge losses to industry.[1] Biocorrosion is a result of synergistic interactions between the various materials surfaces, abiotic corrosion products, bacterial cells and their metabolites.[2] These bacteria typically coexist in naturally occurring biofilms, forming complex colonies on surfaces of various synthetic and natural polymers and structures; irreversible deterioration of properties takes place.[3,4] Large-scale dissemination of microorganisms can cause epidemiologically dangerous situations.

Thus, there is a significant interest in the development of methods for reducing growth and dissemination of detrimental microorganisms.[5–11] Materials science, biomedical industry as well as protection of cultural heritage are all involved. A promising area in this respect are hybrid composites which by definition contain inorganic as well as organic constituents. Diverse molecular structures (polymers, organic and organometallic compounds, biomolecules, inorganic clusters, etc.) are combined in various ratios. By controlling their mutual arrangement, they can be used for a variety of purposes such as bone cements, antibacterial polymer coatings, self-adhesive polymers, and more, while trying to achieve synergic behavior.[5–8,10–17]

The objective of the present work is the development of new hybrid materials with antibiocorrosion capability. Apparently polyfunctional heterochain organic polymers, such as polyurethane elastomers, polyurethane-acrylates or ionomers can be used as matrices for creation of antibiocorrosion coatings.[18,19] Epoxy resins can also be used for the purpose, as can be ferrocene containing composites. These facts constituted the starting point for the present work.

Experimental methods

Differential scanning calorimetry (DSC) was used above all to locate the phase transitions. The technique has been well described by Menard.[20] We have used a DSC 200 apparatus from Netzsch, Selb, Germany. All tests were conducted under dry nitrogen from -100°C up to $+300^{\circ}$C at the heating rate of 5°C min^{-1}.

Thermogravimetric analysis (TGA) is also well described by Menard.[20] We have used a MOM apparatus, model Q1500D, from Budapest. Approximately 100 mg of each dried sample was heated over the temperature range from $+30$ to $+700^{\circ}$C at the heating rate of 10°C min^{-1}.

Important for intended applications are tribological properties, as reviewed in.[21–23] Dynamic friction and wear were determined under sliding conditions by using a Nanovea pin-on-disk tribometer from Micro Photonics Inc. The friction was determined during the test by measuring the friction force by means of the

[1]Laboratory of Advanced Polymers & Optimized Materials (LAPOM), Department of Materials Science and Engineering and Department of Physics, University of North Texas, 3940 North Elm Street, Denton TX 76207, USA
[2]Institute of Inorganic-organic Hybrid Compounds and Non-traditional Materials, College of Exact and Natural Sciences, Ivane Javahishvili Tbilisi University, 3 Ilia Chavchavadze Avenue, 0179 Tbilisi, Georgia

*Corresponding author, email wbrostow@yahoo.com

Received 30 August 2014; accepted 24 October 2014
DOI 10.1179/1433075X14Y.0000000256

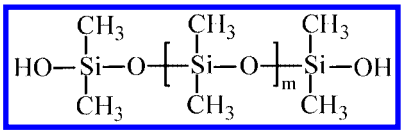

1 Chemical structure of bis(hydroxyalkyl)polydimethylsiloxane

deflection of an elastic arm serving as a force sensor. Rotations of the disk are driven by a servo motor providing up to 500 rev min^{-1}. Pins made from 440 Steel made by Salem Specialty Balls with the diameter of 3·2 mm were used. The tests we performed under the following conditions: temperature 20 ± 2°C, speed 100 rev min^{-1}, radius 2·0 mm, load 2·0 N (for PEU and the respective hybrids) and 5·0 N (for ED-20 epoxy and hybrids based on it). The number of revolutions was 2000 (for PEU) and 3000 (for ED-20). The test durations ranged between 20 and 30 min.

We have determined scratch resistance using a Micro-Scratch Tester (MST) from CSM, Peseux, Switzerland. We have applied a linearly increasing force from 0 to 30·0 N for a distance of 5·0 mm. A minimum of 10 scratches were performed for each sample at the scratch speed of 5·0 mm min^{-1}. The conical diamond intender had a diameter of 200 μm and a cone angle of 120°. The error bars on residual depth are around ±3 μm while for the penetration depth they are around ±9 μm. We have so determined the instantaneous or penetration depth R_p and the residual (healing) depth R_h two minutes after the passage of the indenter.

The sliding wear determination (SWD) was performed by multiple scratching along the same groove using the same MST. Again, each time the penetration depth R_p and the healing depth R_h two minutes after the passage of the indenter were determined.

An environmental scanning electron microscope (ESEM) from FEI, Quanta 200 model, was used to observe the surface morphologies.

Development of composites

We started by working with an ED-20 epoxy made in the Institute of Polymeric Materials in Sumgaiyt, Azerbaijan. ED-20 is made starting with reacting two moles of epichlorohydrin with one mole of bisphenol A to form the bisphenol A diglycidyl ether (commonly abbreviated to DGEBA or BADGE). DGEBA resins are transparent colorless-to-pale-yellow liquids at room temperature, with viscosity typically in the range of 5–15 Pa s at 25°C. The epoxy number e.n.=20, the number of epoxy equivalents in 1 kg of resin. We have also similarly worked with a polyester urethane (PEU) based on 4,4-dimethylmethanediisocyanate and oligobuthyleneglycoladipinate. The neat polymers turned out to have relatively low thermal stability, on heating they exhibited cracking and changing colour to yellow. Advance information suggested non-volatility, low surface tension, hydrophobicity and high resistance to thermal oxidation and visible light of a silicon organic oligomer, namely α,ω-dihydroxyoligodimethylsiloxane, to be also called below bis(hydroxyalkyl) polydimethylsiloxane; its structure is shown in Fig. 1, with $m=15$.

The material shown in Fig. 1 appeared usable as a modifier for epoxies. As bioactive components for antibiocorrosion coatings we used bis(η^5-cyclopentadienyl)iron (better known as ferrocene) bound with an asymmetric polycarbocyclic fragment of adamantane (Fig. 2, X) or else its coordination compounds with cobalt and nickel (Fig. 2, Y, Z). Details of the respective synthesis have been described earlier by some of us.[24]

Hybrids have been created on the basis of the following considerations. Less than 3 wt-% of a bioactive compound was insufficient to achieve desired properties. Further, we have found that more than 10 wt-% of the additive resulted in lowering mechanical parameters. Thus, we have used 3, 5 or 10 wt-% of each of the additives. The compositions of the hybrids studied are displayed in Tables 1 and 2.

When epoxy is the basis, we mix the epoxy and 3, 5 or 10 wt-% the silicon organic oligomer for 30 min at room temperature in the presence of hexamethylenediamine as the hardener and then add 5 wt-% of the bioactive component.

When PEU is the basis, we add 3 or 5 wt-% the modifier and 5 wt-% of the bioactive components to a cyclohexanone solution of PEU under stirring at 155°C until formation of a light colour homogenous mass.

The antibiocorrosion materials so prepared are deposited as smooth coatings on a variety of substrates, including wood and Teflon. The resulting composites are hardened and dried for 48–72 h at room temperature.

Thermophysical properties

DSC results show that all materials studied are amorphous, melting transitions are not visible. We do not include the DSC diagrams for brevity. We recall the statement of Kalogeras and Hagg Lobland about the

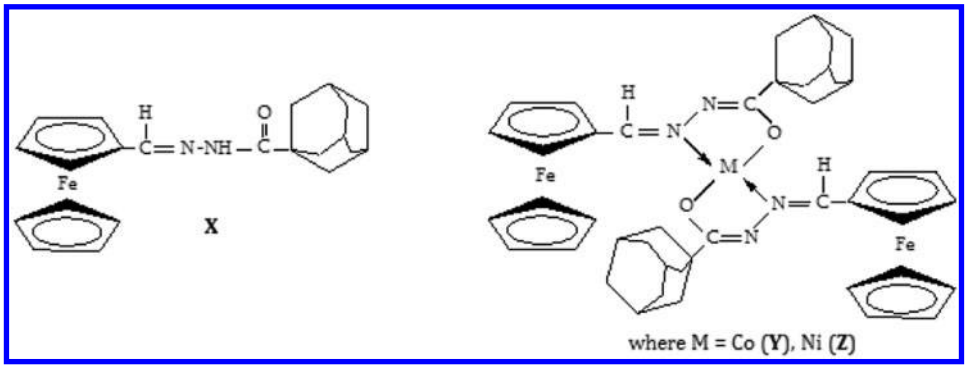

2 Formylferrocenyl-N-(1-adamantoyl) hydrazone and coordination compounds used

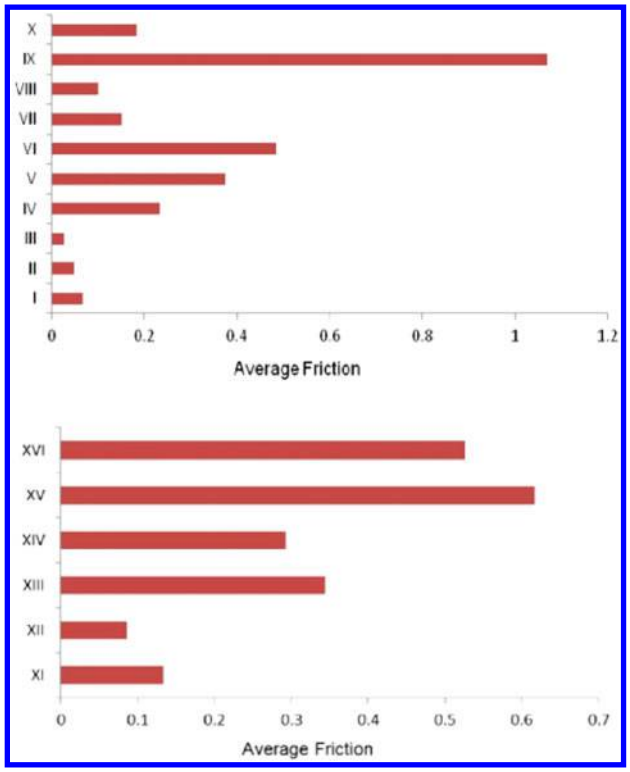

3 Average dynamic friction results; symbols are explained in Tables 1 and 2

increasing importance of non-crystalline solids.[25] All our materials have glass transition regions above $+50^{\circ}C$. Glass transition temperatures are listed in Table 3. This is important for the use of our coatings in museum exhibits since optical clarity is assured at room temperature, or more generally in the service temperature range.

DSC diagrams show also phase transitions in the glassy state, so called β transitions. As discussed by Gedde,[26,27] significant changes occur with time in the glassy state. β transitions are usually assigned to local segmental relaxations including side group motions. Some authors claim that crankshaft motions (four segments minimum) belong here, while a considerable swept-out volume is involved. β transitions are known to take place also in comb polymer liquid crystals, as discussed by Schönhals *et al.*[28]

Going from composite I to II we see that adding of 3 wt-% bis(hydroxyalkyl) polydimethylsiloxane to ED-20 results in lowering the beta transition temperature T_β from -47 to $-57^{\circ}C$. Apparently the internal cohesion of the low temperature neat epoxy is perturbed by the presence of siloxane. On the other hand, composite VI has $T_\beta = -44^{\circ}C$. Thus, the addition of cobalt containing coordination compound enhances the stability of the low temperature amorphous phase.

We now consider TGA results. Up to $200^{\circ}C$ our epoxy and hybrids based on it are quite stable; the weight at $200^{\circ}C$ is 94·6% of the original weight. A large weight drop is seen at 410–$430^{\circ}C$; the remaining weight is about 22% of the original weight. This applies to both neat polymers and hybrids; apparently the presence of additives to the epoxy affects thermal degradation only insignificantly.

As for PEU based hybrids, the remaining weight seen in TGA at $200^{\circ}C$ is even higher, 97·2%. At $330^{\circ}C$ the remaining weight amounts to 35%.

Following work by Travinskaia and her colleagues,[29] we have also determined hydrophobicity by TGA during 720 h at room temperature. Water absorption ability depends on the content of silicon-organic modifier, namely it decreases when increasing the modifier concentration. Water absorption does not exceed 0·03 wt-% in all cases.

Tribological properties

We report first the dynamic friction results obtained with the pin-on-disk tribometre. The standard deviation of the measurements is $\pm 0{\cdot}035$. These results are summarised in Fig. 3.

Consider first the top part of Fig. 3, that is the epoxy (I) and hybrids based on it. Materials II and III which contain bis(hydroxyalkyl)polydimethylsiloxane have lower dynamic friction than the pure epoxy. Addition of the bioactive components increases friction significantly.

The bottom part of Fig. 3 has a different horizontal scale than the top part; values as high as for epoxy based hybrids are not seen. However, also here addition of the bioactive components results in a friction increase. Complex structures of these components seen in Fig. 2 seem to be responsible.

Table 2 Materials based on PEU polyurethane

Symbol	Composition
XI	PEU neat (without fillers or additives)
XII	PEU + 3% bis(hydroxyalkyl)polydimethylsiloxane
XIII	PEU + 3% bis(hydroxyalkyl)polydimethylsiloxane + 5%X
XIV	PEU + 5% bis(hydroxyalkyl)polydimethylsiloxane + 5%X
XV	PEU + 3% bis(hydroxyalkyl)polydimethylsiloxane + 5%Z
XVI	PEU + 5% bis(hydroxyalkyl)polydimethylsiloxane + 5%Z

Table 1 Materials based on ED-20 commercial epoxy

Symbol	Composition
I	ED-20 neat (without fillers or additives)
II	ED-20 + 3% bis(hydroxyalkyl)polydimethylsiloxane
III	ED-20 + 5% bis(hydroxyalkyl)polydimethylsiloxane
IV	ED-20 + 3% bis(hydroxyalkyl)polydimethylsiloxane + 5%X
V	ED-20 + 5% bis(hydroxyalkyl)polydimethylsiloxane + 5%X
VI	ED-20 + 3% bis(hydroxyalkyl)polydimethylsiloxane + 5%Y
VII	ED-20 + 5% bis(hydroxyalkyl)polydimethylsiloxane + 5%Y
VIII	ED-20 + 10% bis(hydroxyalkyl)polydimethylsiloxane
IX	ED-20 + 10% bis(hydroxyalkyl)polydimethylsiloxane + 5%X
X	ED-20 + 10% bis(hydroxyalkyl)polydimethylsiloxane + 5%Y

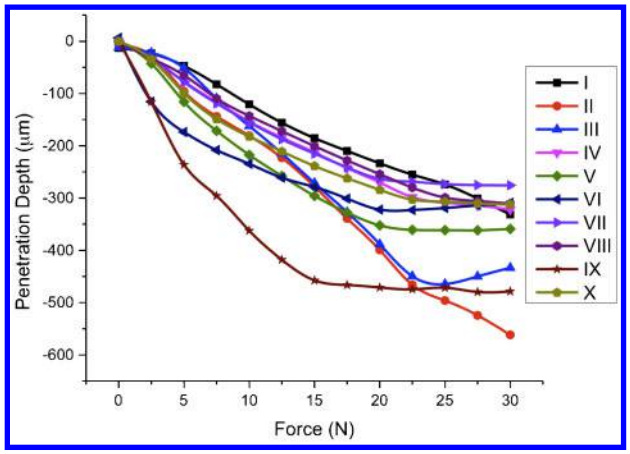

4 Single scratch penetration depths of neat epoxy and respective hybrids as function of applied force

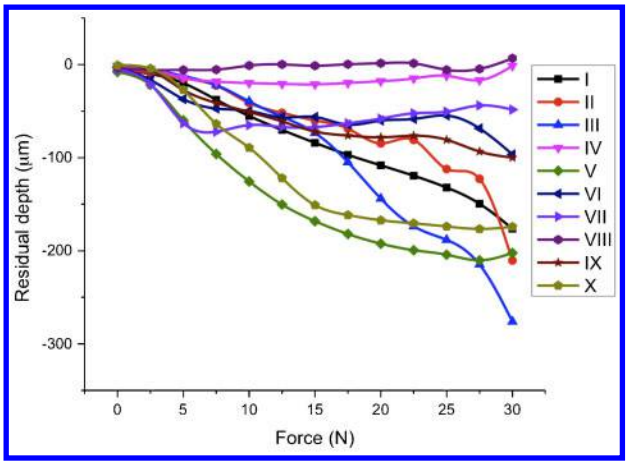

5 Single scratch recovery depths of neat epoxy and respective hybrids as function of applied force

We now consider scratch resistance results for epoxy based hybrids. The instantaneous depth recorded at a given location at the time of the passage of the indenter is the penetration depth R_p. Within 2 min viscoelastic recovery takes place, and the final residual or healing depth R_h is recorded.[21,23] Values reported here are averages, each for a series of five runs for a given kind of material. We display penetration depths for epoxy based hybrids in Fig. 4 and recovery depths in Fig. 5.

There are two significant findings. First, the penetration depth for the pure epoxy is shallower than most of the hybrids. However, the healing depth for most hybrids is shallower than for the neat epoxy. Since the recovery occurs within two minutes, this is an important result. Clearly the best recovery is seen in materials VIII and IV.

We have also performed sliding wear determination as described in the section 'Experimental methods'. That is, one performs consecutive scratching runs along the same groove. For brevity we display selected residual depths in Fig. 6.

Except for hybrid III, other hybrids have shallower healing depths than the neat epoxy. Thus, also in sliding wear, the hybrid formation enhances the scratch resistance. We also observe the tendency towards a horizontal asymptote with increasing number of scratches along the same groove. This is the strain hardening in sliding wear discovered earlier in several polymers.[30] Polystyrene does not show strain hardening in sliding wear, which was one of the motivations for formulating an equation defining brittleness of materials,[31] an equation now widely used.[32]

It would be difficult to derive generalised conclusions on epoxy based versus polyurethane based composites. As can be seen in Fig. 3, we have the lowest friction value for an epoxy based composite. However, the highest friction value is also seen for an epoxy based composite. We conclude that the polymeric matrix does not have a decisive role in defining the properties. A combination of factors determines a property. Thus, the highest dynamic friction value is seen for composite IX which contains the additive X (see again Fig. 2). However, when we now focus on polyurethane based composites, we find that composites XIII and XIV – which also contain the additive X – do not exhibit the highest friction values in the PEU class. Overall, PEU surfaces are known to be softer than those of epoxies, hence higher wear resistance of the latter.

Table 3 Glass transition temperatures

Symbol	T_g/°C	Symbol	T_g/°C
I	76	VI	58
II	60	VII	54
III	59	VIII	56
IV	58	IX	42
V	40	X	35

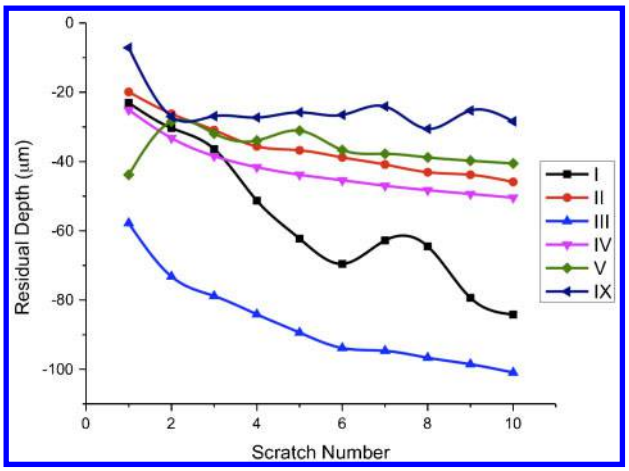

6 Residual depths of neat epoxy and selected hybrids at constant force 5·0 N as function of scratch number

Surface morphology

Since tribological properties depend on the contacting surfaces, we have observed the surface morphology and changes in the wear track surface after pin-on-disk tribological testing by SEM. The results for epoxy based hybrids and for polyurethane based hybrids are presented, respectively, in Figs. 7 and 8.

Micrographs in Fig. 7 actually speak for themselves. Hybrids IV, V, VII and VIII have more wear resistant surfaces. The almost defect-free look of micrographs for materials IV and V fits well with the residual depth

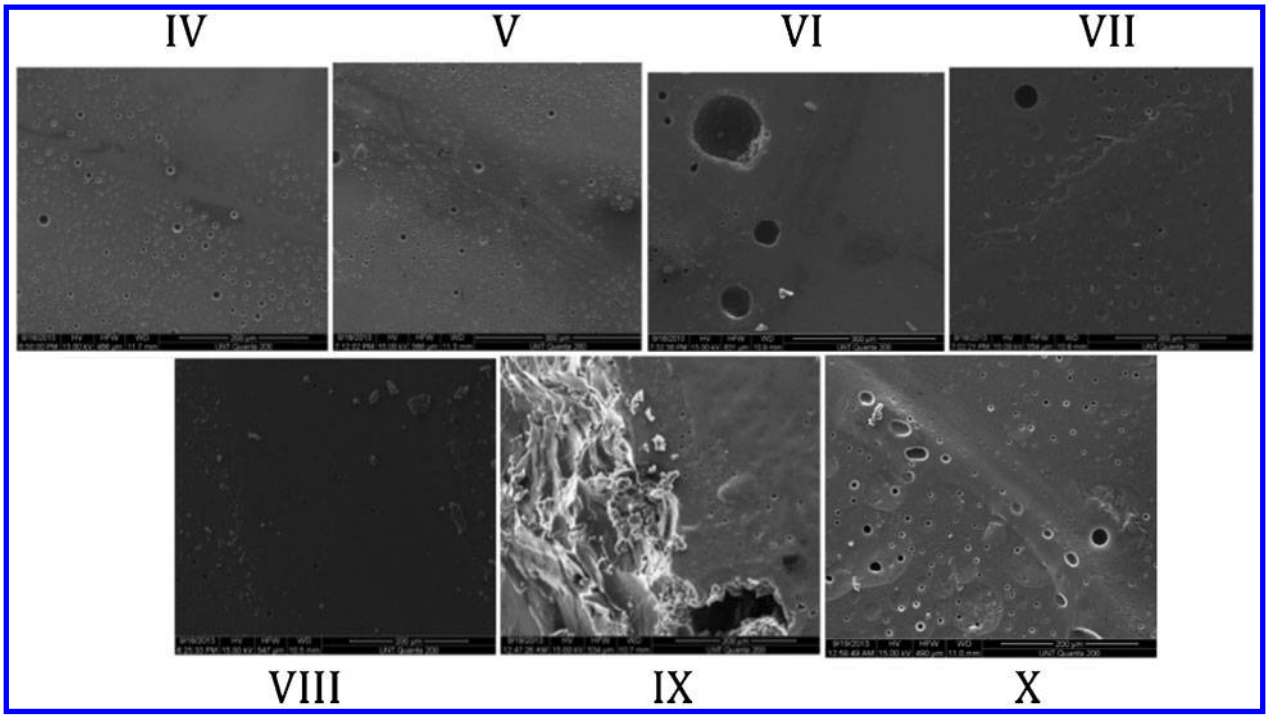

7 SEM micrographs of epoxy based hybrid coatings at 200 μm

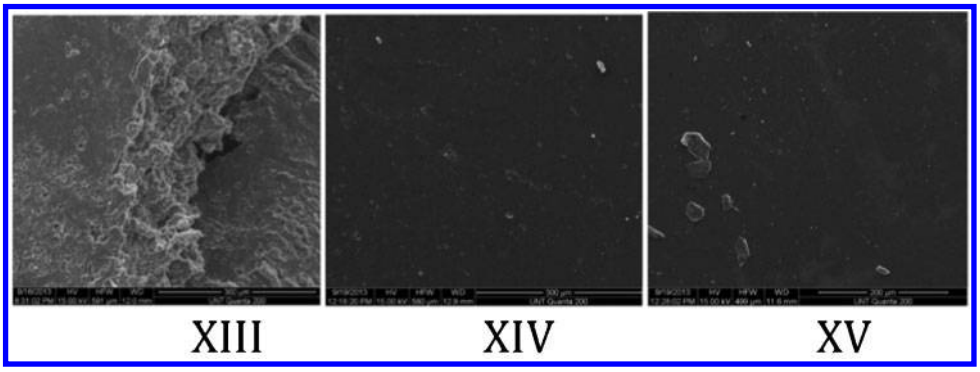

8 SEM micrographs for PEU based hybrid coatings at 200 μm

curves in sliding wear determination for these materials in Fig. 6. While sample IX has significantly higher residual depth in Fig. 6, we see the irregular character of that curve – reflected also in the uneven surface structure in Fig. 7. Figure 8 shows that hybrid XIV has high scratch resistance.

Finally, samples subjected to three months aging under normal temperature and pressure conditions were observed. The initial colours, homogeneity of the surface and optical transparency were preserved. No phase separation took place. Photographs for four of them are shown in Fig. 9.

Antibiocorrosion efficacy of our hybrids will be reported in a separate paper. As discussed by Stavinskaya and her colleagues,[33] there is a large variety of bioactive materials, including vitamins, cosmetics and also extracts from plants.

Acknowledgements

We would like to thank the Shota Rustaveli National Science Foundation (RNSF) of Georgia, Tbilisi, for financial support. Prof. Alexander Fainleib, Institute of

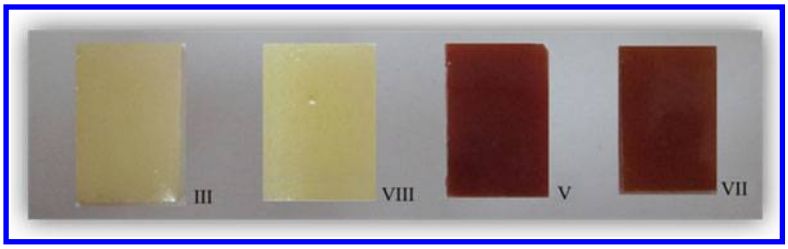

9 Photographs of selected hybrids after three months

Chemistry of Macromolecular Compounds of the Academy of Sciences of Ukraine, Kyiv, has provides us with some of his materials.

References

1. B. Tribollet: 'Electrochemical sensors for biofilm and biocorrosion', *Mater. Corros.*, 2003, **54**, 527.
2. I. B. Beech and J. Sunner: 'Biocorrosion: towards understanding interactions between biofilms and metals', *Curr. Opin. Biotechnol.*, 2004, **15**, 181.
3. P. W. Baker, K. Ito and K. Watanabe: 'Marine prosthecate bacteria involved in the ennoblement of stainless steel', *Environ. Microbiol.*, 2003, **5**, 925.
4. T. Zhang, H. H. P. Fang and B. C. B. Ko: 'Methanogen population in a marine biofilm corrosive to mild steel', *Appl. Microbiol. Biotechnol.*, 2003, **63**, 101.
5. J. D. Gu: 'Microbiological deterioration and degradation of synthetic polymeric materials: recent research advances', *Int. J. Biodeterior. Biodegr.*, 2003, **52**, 69–91.
6. Proc. 41st IUPAC World Chemistry Congress on 'Chemistry of the protection of health, natural environment and cultural heritages', Torino, Italy, August 2007, IUPAC.
7. A. W. Wren, M. N. Cummins and M. R. Towler: 'Comparison of antibacterial properties of commercial bone cements and fillers with a zinc-based glass polyalkenoate cement', *J. Mater. Sci.*, 2010, **45**, 5244–5251.
8. O. Clarkin, A. W. Wren, R. Thornton, J. Cooney and M. Towler: 'Antibacterial analysis of a zinc-based glass polyalkenoate cement', *J. Biomater. Appl.*, 2011, **26**, 277–292.
9. M. E. Tousley, A. W. Wren, M. R. Towler and N. P. Mellott: 'Processing, characterization and bactericidal activity of undoped and silver-doped vanadium oxides', *Mater. Chem. Phys.*, 2012, **137**, 596–603.
10. B. Oktay and N. Kayaman-Apohan: 'Polydimethylsiloxane (PDMS)-based antibacterial organic-inorganic hybrid coatings', *J. Coat. Technol. Res.*, 2013, **10**, 785–798.
11. S. B. Heo, Y. S. Jeon, Y. J. Kim, S. H. Kim and J.-H. Kim: 'Bioinspired self-adhesive polymer for surface modification to improve antifouling property', *J. Coat. Technol. Res.*, 2013, **10**, 811–819.
12. J. Thome, A. Hollander, W. Jaeger, I. Trick and C. Oehr: 'Ultrathin antibacterial polyammonium coatings on polymer surfaces', *Surf. Coat. Technol.*, 2003, **174–175**, 584–587.
13. J. H. Oh, Y. G. Kim and D. G. Lee: 'Optimum bolted joints for hybrid composite materials', *Compos. Struct.*, 1997, **38**, 329–341.
14. A. P. Mouritz, E. Gellert, P. Burchill, K. Challis: 'Review of advanced composite structures for naval ships and submarines', *Compos. Struct.*, 2001, **53**, 21–42.
15. M. V. Hosur, M. Adbullah and S. Jeelani: 'Studies on the low-velocity impact response of woven hybrid composites', *Compos. Struct.*, 2005, **67**, 253–262.
16. P. Gomez-Romero and C. Sanchez: 'Functional hybrid materials', 2006, Weinheim, Wiley-VCH.
17. I. C. Finegan and R. F. Gibson: 'A review of recent research on mechanics of multifunctional composite materials and structures', *Compos. Struct.*, 2010, **92**, 2793–2810.
18. U. V. Savelyev, E. R. Akhranovich, A. P. Grekov, E. G. Privalko, V. V. Korskanov, V. I. Shtompel, V. P. Privalko, P. Pissis and A. Kanapitsas: 'Influence of chain extenders and chain end groups on properties of segmented polyurethanes: I. Phase morphology', *Polymer*, 1998, **39**, 3425–3429.
19. P. Pissis, A. Kanapitsas, U. V. Savelyev, E. R. Akhranovich, E. G. Privalko and V. P. Privalko: 'Influence of chain extenders and chain end groups on properties of segmented polyurethanes: II. Dielectric study', *Polymer*, 1998, **39**, 3431–3435.
20. K. P. Menard: in 'Performance of pastics', (ed. W. Brostow), Ch. 8; 2000, Munich–Cincinati, Hanser.
21. W. Brostow, J.-L. Deborde, M. Jaklewicz and P. Olszynski: 'Tribology with emphasis on polymers: Friction, scratch resistance and wear', *J. Mater. Ed.*, 2003, **25**, 119–132.
22. N. K. Myshkin, M. I. Petrokovets and A. V. Kovalev: 'Tribology of polymers: friction, wear and mass transfer', *Tribol. Int.*, 2005, **38**, 910–921.
23. W. Brostow, V. Kovacevic, D. Vrsaljko and J. Whitworth: 'Tribology of polymers and polymer based composites', *J. Mater. Ed.*, 2010, **32**, 273–290.
24. Kh. Barbakadze, G. Lekishvili and N. Lekishvili: 'Adamantane-containing biologically active compounds: synthesis, properties and use', *Asian J. Chem.*, 2014, **26**, 1315–1317.
25. I. M. Kalogeras and H. E. Hagg Lobland: 'The nature of the glassy state: Structure and transitions', *J. Mater. Ed.*, 2012, **34**, 69–94.
26. S. M. Gubanski, K. Karlsson and U. W. Gedde: in Conference Record of 1992 IEEE Int. Symp. on 'Electrical insulation', Baltimore, MD, USA, June 1992, IEEE.
27. U. W. Gedde: 'Polymer physics'; 2001, Dordrecht–Boston Kluver.
28. A. Schönhals, D. Wolff and J. Springer: *Macromolecules*, 1995, **28**, 6254–6257.
29. T. A. Travinskaia, E. A. Mishuk, L. N. Perepelitisina and Yu. V. Savyelev: 'Obtaining and properties of biodegradable materials based on ionomer polyurethane and polysaccharide', *Polimernyi Zh.*, 2010, **32**, 66–74.
30. W. Brostow, G. Damarla, J. Howe and D. Pietkiewicz: 'Determination of wear of surfaces by scratch testing', *e-Polymers*, 2004, 025.
31. W. Brostow, H. E. Hagg Lobland and M. Narkis: 'Sliding wear, viscoelasticity and brittleness of polymers', *J. Mater. Res.*, 2006, **21**, 2422–2428.
32. W. Brostow, H. E. Hagg Lobland and M. Narkis: 'The concept of materials brittleness and its applications', *Polymer Bull.*, 2011, **59**, 1697.
33. O. Stavinskaya, I. Laguta and I. Orel: 'Silica-gelatoin composite materials for prolonged desorption of bioactive compounds, *Mater. Sci. Medziagotyra*, 2014, **20**, 171–176.